



**Semi-continuous anaerobic co-digestion of vegetable waste and cow manure: a study of process stabilization**

**Co-digestión anaerobia en modo semi-continuo de residuos de vegetales y estiércol de vaca: un estudio de estabilidad de proceso**

L. R. Miramontes-Martínez<sup>1,3</sup>, R. Gomez-Gonzalez<sup>1</sup>, J. E. Botello-Álvarez<sup>2</sup>, C. Escamilla-Alvarado<sup>1,3</sup>,  
A. Albalate-Ramírez<sup>1,3</sup> and P. Rivas-García<sup>1,3\*</sup>

<sup>1</sup>*Departamento de Ingeniería Química, Facultad de Ciencias Químicas, Universidad Autónoma de Nuevo León, Av. Universidad S/N, Cd. Universitaria, 64451, San Nicolás de los Garza, Nuevo León, Mexico.*

<sup>2</sup>*Doctorado en Ciencias de la Ingeniería, Departamento de Ingeniería Bioquímica, Instituto Tecnológico de Celaya, Av. Tecnológico y A. García Cubas, 38010, Celaya, Guanajuato, Mexico.*

<sup>3</sup>*Centro de Investigación en Biotecnología y Nanotecnología, Facultad de Ciencias Químicas, Universidad Autónoma de Nuevo León, Parque de Investigación e Innovación Tecnológica, km 10 Highway to the International Airport Mariano Escobedo, 66629, Apodaca, Nuevo León, Mexico.*

Received: October 9, 2019; Accepted: December 15, 2019

**Abstract**

The anaerobic digestion of vegetable waste (VW) often shows the accumulation of fatty acids and low buffering capacity that promotes instability and low methane productivity. This work evaluated the anaerobic co-digestion of VW with cow manure (CM) as a strategy to improve the process stability. As a reaction system, a 4 L semi-continuous stirred tank reactor with an HRT of 20 days and fed with a substrate formulation of 40 g of VS was used in two periods: 34 days of VW mono-digestion and 26 days of VW:CM co-digestion. The mono and co-digestion processes were numerically evaluated through three analysis tools: a proposed co-digestion model embedded in the *Anaerobic Digestion Model No. 1* structure, statistical process control theory, and modeling the pH dynamics as the response of a first-order linear system to an impulse manipulation. The mono-digestion process showed yields of 0.381 L CH<sub>4</sub> L digester<sup>-1</sup>d<sup>-1</sup>, which increased by 14% during co-digestion. The results indicated that in VW:CM co-digestion the pH had a slower dynamical response to the daily pulse feed, keeping the pH within the statistical stability range. The early warning indicator IA/BA (ratio between intermediate and bicarbonate alkalinity) also stayed away from the failure threshold. It was shown that the addition of CM to a mono-digestion of VW increases the buffer capacity of the system and the production of CH<sub>4</sub>, promoting a stable and efficient process.

*Keywords:* Anaerobic co-digestion; vegetable waste; cow manure; *Anaerobic Digestion Model No. 1*; process stability.

**Resumen**

La digestión anaerobia de los residuos vegetales (VW) a menudo muestra una acumulación de ácidos grasos volátiles y una baja capacidad de amortiguación que promueve la inestabilidad y la baja productividad de metano. Este trabajo evaluó la co-digestión anaerobia de VW con estiércol de vaca (CM) como una estrategia para mejorar la estabilidad del proceso. Como sistema de reacción, se usó un reactor de tanque agitado semi-continuo de 4 L con un HRT de 20 días y alimentado con una formulación de sustrato de 40 g de VS en dos períodos: 34 días de mono-digestión VW y 26 días de co-digestión VW:CM. Los procesos de mono y co-digestión se evaluaron numéricamente a través de tres herramientas de análisis: un modelo de co-digestión propuesto e integrado en la estructura del *Anaerobic Digestion Model No. 1*, teoría de control de procesos estadísticos y modelado de la dinámica del pH como respuesta de un sistema lineal de primer orden a un impulso. El proceso de mono-digestión mostró una productividad de 0.381 L CH<sub>4</sub> L digester<sup>-1</sup>d<sup>-1</sup>, que aumentó en un 14% durante la co-digestión. Los resultados también indicaron que en la co-digestión VW:CM la dinámica del pH presenta una respuesta más lenta a la alimentación diaria inducida por pulsos, manteniendo los valores de este parámetro dentro del rango de estabilidad estadística; así como el indicador de alerta temprana IA/BA (relación entre alcalinidad intermedia y bicarbonatos) fuera de los umbrales de falla. Se demostró que la adición de CM a un proceso mono-digestión de VW aumenta la capacidad de amortiguación del sistema y la productividad de CH<sub>4</sub>, promoviendo un proceso estable y eficiente.

*Palabras clave:* Co-digestión anaerobia; residuos vegetales; estiércol de vaca; *Anaerobic Digestion Model No. 1*; estabilidad de proceso.

\* Corresponding author. E-mail: pasiano.rivasgr@uanl.edu.mx  
Tel. (81) 8329-4000 Ext. 3427  
<https://doi.org/10.24275/rmiq/proc920>  
issn-e: 2395-8472

## 1 Introduction

---

The global growth in the production of fruits and vegetables is over 1730 Gt year<sup>-1</sup>, out of which it is estimated that 15% of the fruits and 25% of the vegetables are wasted (FAO, 2014). Around 35% of the FVW are generated during the processing and distribution of fruits and vegetables (FAO, 2011). These are caused by the quality standards required by the customers, shortage of processing capacity, and storage costs (Zeynali *et al.*, 2017). Wholesale markets and supply centers are the primary sources of FVW. For instance, Mexico City has one of the biggest wholesale markets in the world, generating 447 t FVW d<sup>-1</sup> (CEDA, 2011).

Regulations around the world mandate the FVW to be disposed at sanitary landfills, incineration centers, anaerobic digesters, and composting (Gavilán *et al.*, 2018). The disposal of FVW can have a harmful impact on the waste treatment processes: *e.g.*, FVW fosters an unstable combustion in the incineration chambers creating an environment conducive to dioxins production (Hartmann and Ahring, 2006); in landfills, FVW increases the production of lixiviates and greenhouse gas emissions (Escamilla-Alvarado *et al.*, 2017). This latter technology is responsible for the generation of 384 Mt of CO<sub>2</sub> eq year<sup>-1</sup> just in Mexico (Breeze, 2018). These problems are associated with the high organic matter content (>95% on dry basis) and humidity (>80%) of the FVW (Cheng and Hu, 2010). Indeed, regulations such as the European Landfill Directive 99/31/EC mandate avoiding the disposal of biodegradable wastes to landfills (Escamilla-Alvarado *et al.*, 2017).

Alternatives for the disposal of FVW include the anaerobic digestion (AD), a treatment that has a high potential of energy recuperation (Aldana-Espitia *et al.*, 2017; De Baere, 2006; Flores-Estrella *et al.*, 2016; Kafle *et al.*, 2014; Rivas-García *et al.*, 2015). The AD takes place in a molecular-oxygen free environment where, under symbiotic and syntrophic conditions, several microbial groups degrade organic matter, generating biogas and digestate as the final products. The biogas can be used as fuel for electricity production and the digestate as soil enhancer (Abubaker *et al.*, 2012; Tambone *et al.*, 2010).

Several studies had emphasized the fact that the AD of FVW and vegetable waste (VW) operates in a stable regime only at low organic load rates (OLR).

Knol *et al.* (1978) established that the maximum OLR for the AD of VW is 1.6 g VS L<sup>-1</sup>d<sup>-1</sup>, with a biogas yield of 0.30 - 0.58 L g VS<sup>-1</sup>. The instability of the AD of wastes is commonly associated with the accumulation of volatile fatty acids (VFA) and low buffering capacity of the reactive system. The hydrolysis of organic matter generated the VFA via catabolic reactions, such as the acidogenesis and acetogenesis of soluble substrates (García-Peña *et al.*, 2011; Masebinu *et al.*, 2018; Scano *et al.*, 2014). These phenomena caused a decrease in the pH of the process, thus inhibiting the methanogenic biomass (Mata-Alvarez *et al.*, 1992).

Recent literature reported that to improve the conditions of the process and increase the CH<sub>4</sub> yield in the AD of VW and FVW, a co-substrate should be used (Chakraborty and Mohan, 2018; Di Maria *et al.*, 2015; Li *et al.*, 2017; Matheri *et al.*, 2017; Pavi *et al.*, 2017; Wang *et al.*, 2018). The process of co-digestion offers several benefits, such as *i*) dilution of inhibitory species (Mata-Alvarez *et al.*, 2014; Astals *et al.*, 2014), *ii*) higher nutrient availability, which could increase the biodegradability, and *iii*) changes in the microbial flora that could result in enhanced metabolic performance (Ebner *et al.*, 2016).

Jiang *et al.* (2012) studied the AD of VW in a continuous stirred tank reactor (CSTR). Their results indicated that using VW as the only substrate was not advisable for an AD process. Due to an inhibitory process as a result of the accumulation of VFA and the decrease of pH in the reactor. The authors pointed out that the addition of buffering solutions was not enough to keep the pH from decreasing, whereas the addition of cow manure (CW) in the feed was successful in stabilizing the process. Lin *et al.* (2011) looked into the co-digestion of FVW with food waste (FW) in a CSTR with an OLR of 3 g VS L<sup>-1</sup>d<sup>-1</sup>. They found that the ideal feed ratio is 1:1 on a VS basis, achieving a yield of 0.49 L CH<sub>4</sub> g VS<sup>-1</sup> and that the process exhibited a natural pH control, and stable biogas yield.

The AD process buffering capacity depends mainly on the concentration of N-NH<sub>3</sub>. To improve the relatively low concentration of ammoniacal nitrogen in VW (0.2 mg kg<sup>-1</sup>), Li *et al.* (2014), proposed adding manure as co-substrate, due to its high NH<sub>3</sub> concentration. The authors affirmed that the instability of the AD of VW was a direct result of the high sugars concentration and low N-NH<sub>3</sub> content. The co-digestion with CM makes up for this deficiency, increasing the buffering capacity of the reactive media.

Besides improving critical parameters of the AD process, such as biogas productivity and hindering

inhibitory phenomena, a good co-substrate should promote stabilization in the reactive medium. One of the key challenges for all AD processes is the effective monitoring and diagnostic of the parameters that have a direct impact on the process stability. Li *et al.* (2017) studied the AD of FW in a CSTR. They found that the concentrations of VFA and the ratio of bicarbonate alkalinity to total alkalinity (BA/TA) reflected the biomass metabolic behavior in the digester. Thus effectively serving as early warning indicators. The authors also mentioned that the primary source of AD's alkalinity is ammonia, which reflected the system buffering capacity. Only a few research works had investigated how the yield and productivity of CH<sub>4</sub> are enhanced via the addition of manure in the AD of VW. Specifically how the addition of this substrate impacts the reactive media stability parameters that help to identify problems in the system and that are susceptible to being controlled, such as pH and alkalinity.

The mathematical models play a fundamental role in the study of complex substrates in co-digestion. Nowadays, one of the most sophisticated mathematical models to describe this process is the Anaerobic Digestion Model No. 1 (ADM1), developed by Batstone *et al.* (2002). The ADM1 elucidates the phenomena of the system that are only observable via expensive and complicated experimental techniques, *e.g.*, the continuous measuring of VFA in the effluent, the biogas characterization, and the dynamics of the microorganisms groups. Despite its level of sophistication, the ADM1 could not model the co-digestion processes accurately since it models the organic matter as a single variable with constant proximal composition and average biodegradability. This assumption limits its modeling capacity of co-digestion processes since the co-substrates are heterogeneous, and the organic matter in the reactive media has a dynamic composition.

Several extensions and modifications had been incorporated into the structure of the ADM1 to consider the co-digestion process. Zaher *et al.* (2009) developed the general integrated solid waste co-digestion (GISCOD) model based on ADM1. This model considers the hydrolysis of each substrate separately, ignoring the disintegration step. The authors used their model on the CM and kitchen waste co-digestion, getting useful simulation results that helped optimize the process. García-Gen *et al.* (2015) developed a methodology to estimate the kinetic parameters for disintegration and hydrolysis of solid waste, according to their findings, they

proposed a co-digestion model based on ADM1. In this model, the proximal fractions of the substrate and co-substrate were divided into fast and slow biodegradability fractions. The resulting co-digestion model is relatively easy to implement but is less accurate than the GISCOD model (Xie *et al.*, 2016). The co-digestion models, based on the original ADM1, suffer from the fact that they do not consider the changes in the organic matter proximal composition over time, the influence of the inoculum organic matter, nor its proximal composition at the beginning of the co-digestion run. Additionally, the addition of a considerable number of variables and parameters needed to represent multiple substrates complicates the model implementation. Since a series of hydrolysis parameters must be defined for each constitutive fraction of substrate, namely carbohydrates, proteins, fats, and inert matter.

This paper presents a study of anaerobic co-digestion of VW with CM. The objective is to analyze the stability of the process in mono and co-digestion regimes of VW. A new co-digestion and alkalinity model is proposed based on the structure of ADM1, which was validated with experimental results. As a strategy to evaluate the stability and dynamic behavior of the system, the Shewhart control charts, and the response of the first-order models to impulse disturbances in the feed were used.

## 2 Materials and methods

### 2.1 Substrates and inoculum

Activated sludge from a waste treatment anaerobic reactor from a local brewing company was used as inoculum. The vegetable waste (VW) substrate contained discarded tomatoes, onions, potatoes and carrots, and lettuce scraps from a local supermarket. The VW formulation is shown in Table S1 of the Supplementary material. Dairy cow manure (CM) provided by a farm of Universidad Autonoma de Nuevo Leon was used as co-substrate. Both substrates, the VW and CM, were ground separately in a domestic blender (Proctor Silex®) for 30 min. The concentration of volatile solids (VS) in each substrate was adjusted to 40 g L<sup>-1</sup>. The substrates were sealed in glass flasks and stored at 4 °C.

The substrates, VW and CM, and the inoculum fed into the reactor were characterized via standard physicochemical tests, such as: solids profile (NMX-

F-607-NORMEX-2013), crude fiber (AOAC Official Method 962.09, 1990), crude fat (NMX-AA-005-SCFI-2013), humidity (NOM-116-SSA1-1994), ammonia nitrogen (NOM-242-SSA1-2009), protein (NMX-F-608-NORMEX-2011), total carbohydrates (calculated as the volatile solids minus the amount of protein, crude fat and crude fiber), volatile fatty acids (VFA) and alkalinity (Anderson and Yang, 1992). Daily samples were taken from the reactor and stored at 4 °C in sealed glass flasks, until their characterization via solids profile (NMX-F-607-NORMEX-2013), VFA and alkalinity (Anderson and Yang, 1992), holocellulose (AOAC Official Method, 1998), and ammonia nitrogen (NOM-242-SSA1-2009).

The fraction of methane in the biogas was measured via gas chromatography using a Thermo Scientific (Trace 1310) chromatograph. Equipped with a thermal conductivity detector (TCD) and a column TG-BOND Msieve 5A (30 m x 0.33 mm) molecular sieve TermoFisher Scientific. The temperatures in the oven, the injector, and detector were 100, 150 and 200 °C, respectively. Nitrogen was used as the carrier gas, with a flow of 3 mL min<sup>-1</sup>.

## 2.2 Reaction system

The anaerobic digestion process was performed in an Applikon® reactor equipped with temperature and stirring controllers. The process was operated in a semi-continuous feeding regime, completely stirred, under isothermal conditions, and a constant gas output. The experimental run lasted 60 d, at hydraulic retention time (HRT) of 20 d. The total volume of the reactor is 7 L, out of which 4 L was the operation volume. The reactor mixing was done using a Rushton turbine impeller (60 mm diameter), with a stirring speed of 200 rpm. The reactor temperature of 35 °C was controlled via a heating jacket. The substrates were fed into the reactor via a latex hose and a syringe. Meanwhile, the biogas generated circulated through a water-cooled condenser at 8 °C, to reduce the loss of moisture in the reactor. Finally, the biogas flowed through a Prendo® volumetric flow sensor connected to a 3.8 L sealed bag by a Fisher Scientific® On/Off valve. The biogas was accumulated in the bag, which was replaced daily by an empty bag. The complete experimental system is shown in Figure 1S of the Supplementary material.

The reactor was initially loaded with 3 L of solution at 38 g VS L<sup>-1</sup> of inoculum and 0.2 L of VW. The different feeding periods to the reactor are shown

in Table 2S in the Supplementary material section. During the first period (I, fed-batch regime), 0.2 L of VW were fed daily into the reactor until a total volume of 4 L was reached. This regime promoted the acclimation of the microorganisms to the substrate. For the next two periods, II and III, a semi-continuous operation was followed. The reactive volume was kept constant: 0.2 L were extracted to be analyzed, and the same amount was fed into the reactor. During period II, the reactor operated in a mono-digestion of VW regime that lasted 28 d, while for period III, the co-digestion of VW:CM was 25 d long.

## 2.3 Model development

The Anaerobic Digestion Model No. 1 (Batstone *et al.*, 2002) was used as the basis for modeling the process. Since the ADM1 does not consider the co-digestion in its structure, a modification was developed and added to the original model.

The ADM1 model considers the assumption of perfect mixing and a homogeneous medium that includes dispersed soluble and insoluble species in the same phase. Kinetic expressions are unstructured models that consider the global relationships of the present and measurable species: substrate - microorganism - product. In this particular case, the system is modeled as a tank-type reactor with perfect mixing in semi-continuous operation and with changes in reaction volume ( $V_L$ ). To consider variable volume, an ordinary differential equation, Eq. (1), was introduced. Additionally, all the equations that describe the dynamic behavior of the species present in the liquid phase of the reactor were modified to include this change in volume (Eq. (2)).

$$\frac{dV_L}{dt} = q_{IN} - q_{OUT} \quad (1)$$

$$\frac{desp_i}{dt} = \rho_{esp_i} \left( \frac{V_{L_{t-1}}}{V_L} \right) + \frac{q_{IN}}{V_L} esp_{i,IN} - \frac{q_{OUT}}{V_L} esp_i - \frac{esp_i}{V_L} \frac{dV_L}{dt} \quad (2)$$

where  $V_{L_{t-1}}$  and  $V_L$  are the liquid phases (L) volume before and after feeding the reactor, respectively;  $t$  is the processing time;  $q_{IN}$  and  $q_{OUT}$  are the flow rates in and out of the reactor (L d<sup>-1</sup>);  $esp_{i,IN}$  and  $esp_i$  are the concentration of the  $i$ -th species in the reactor feed and output (g COD L<sup>-1</sup>), respectively. Finally,  $\rho_{esp_i}$  represents the kinetic rate of the  $i$ -th species inside the reactor, as modeled by the ADM1.

The original version of ADM1 assumes that the fractions of insoluble species, such as carbohydrates

( $X_{ch}$ ), proteins ( $X_{pr}$ ), fats ( $X_{li}$ ), and inerts ( $X_i$ ) in the organic matter loaded to the reactor ( $f_{X_{espi},X_c}$ ) and in the feed, are constant during AD. This is an essential simplification of the co-digestion process since depending on the substrates, co-substrates, and inoculum used, the fractions  $f_{X_{espi},X_c}$  could display different values. Additionally, the hydrolysis rates of the organic matter to carbohydrates, proteins, fats, and inert are different, causing variations in the composition of the reactive system.

Several authors recommend separating the organic matter COD in its main components ( $X_{ch}$ ,  $X_{pr}$ ,  $X_{li}$  y  $X_i$ ), as independent inputs to the ADM1. This step effectively omits the organic matter disintegration, and their respective  $f_{X_{espi},X_c}$ , taking the hydrolysis as the controlling step (Nopens *et al.*, 2009; Arnell *et al.*, 2016). The co-digestion models based on the ADM1 take this consideration. The GISCOD model developed by Zaher *et al.* (2009) was based on the premise that enzymes can diffuse through the structure of the different wastes used as substrates. The hydrolysis takes place before the disintegration of the organic matter, and this last step could be omitted. The critical disadvantage of the GISCOD model is the addition of a considerable number of parameters and variables needed to account for multiple substrates requiring the values of the hydrolysis parameters  $X_{ch}$ ,  $X_{pr}$ ,  $X_{li}$ , and  $X_i$  for each substrate (Xie *et al.*, 2016).

In this study, algebraic and differential equations were developed to evaluate the change of the constitutive fractions  $f_{X_{espi},X_c}$  of the organic matter in the reactor. The aim was to model the disintegration of the organic matter in the substrate, co-substrate, and inoculum. As well as including the changes of the organic matter composition in the reactor ( $f_{X_{espi},X_c}$ ), to effectively reduce the number of hydrolysis parameters used in the current co-digestion models. Eqs. (3) - (6) model the co-digestion, where the first three equations represent the substrate and co-substrate mixing process before being fed into the reactor, while Eq. (6) represents the dynamic behavior of  $f_{X_{espi},X_c}$ .

$$espi_{i,IN} = r_{S/Co} espi_{i,S} + (1 - r_{S/Co}) espi_{i,Co} \quad (3)$$

$$X_{C,IN} = r_{S/Co} X_{C,S} + (1 - r_{S/Co}) X_{C,Co} \quad (4)$$

$$f_{X_{espi},X_{CIN}} = \frac{X_{C,S} f_{X_{espi},X_{C(S)}} + X_{C,Co} f_{X_{espi},X_{C(Co)}}}{X_{C,IN}} \quad (5)$$

$$\frac{df_{X_{espi},X_C}}{dt} = \frac{q_{IN} X_{C,IN}}{V_L X_C} f_{X_{espi},X_{CIN}} - f_{X_{espi},X_C} \left[ \frac{1}{V_L} \left( q_{OUT} + \frac{dV_L}{dt} \right) + \frac{1}{X_C} \frac{dX_C}{dt} \right] \quad (6)$$

where  $X_{C,IN}$  is the composite concentration, in g COD  $L^{-1}$ , in the feed;  $r_{S/Co}$  represents the substrate to co-substrate ratio;  $X_{C,S}$  and  $X_{C,Co}$  are the substrate and co-substrate composite concentration, respectively, in g COD  $L^{-1}$ .

The proposed model is made up of ordinary differential equations (ODEs) in the time domain. It describes the dynamic behavior of the species in the liquid phase (Eq. 2), in the gas phase and the structural conformation of the organic matter (Eq 6). The nonlinear algebraic equations allow for the estimation of pH and alkalinity. The ODEs system was solved through the 4th order Runge Kutta method with an integration step of 1E-6 d. In each integration step, the algebraic equations were solved by the bisection method. A numerical validation of the results was done via a dynamic global mass balance implemented alongside the model. The FORTRAN 90 programming language and the Compaq Visual Fortran compiler were used to implement and solve the mathematical structure. More details of the solution methodology are described in Rivas-García *et al.* (2013).

## 2.4 Alkalinity model development

Alkalinity calculation, via ADM1, is a mathematical representation of the experimental determination based on the APHA norms (1992). Sulphuric acid ( $H_2SO_4$ ) at 0.01 N ( $S_{H_2SO_4}$ ) was used as the titration reagent, adding one drop at the time to a sample of 1 mL ( $V_a$ ), until the final pH was reached. A drop volume ( $V_d$ ) of 0.05 mL was considered. Equation (7) is the conventional equation for alkalinity determination.

$$A \text{ mg CaCO}_3 L^{-1} = \frac{V_{H_2SO_4} N_{H_2SO_4}}{V_a} (50)(100) \quad (7)$$

where A is the system's alkalinity;  $V_{H_2SO_4}$  is the volume of sulphuric acid solution used as a reagent; the normality of the solution is represented by  $N_{H_2SO_4}$ ; 50 is the factor needed to convert from eq  $L^{-1}$  to mg  $CaCO_3 L^{-1}$  and the second factor of 1000 converts from mL to L.

The volume of reagent solution,  $V_{H_2SO_4}$ , needed to determine the alkalinity was calculated using the procedure depicted in Figure 2S (in the Supplementary material section) and Eq. (11), which is based on an iterative process that requires the calculation of the pH after each drop of reagent is added to the solution. A global charge balance of the ionic species was used to estimate the molar concentration of hydronium ions, Eq. (8), which in turn define the pH of the solution (the nomenclature of this equation is the same that the ADM1 use, Batstone *et al.* (2002)). The ionic species came from the soluble compounds in Eq. (2), the molar balances, the physicochemical equilibrium relationships, and the concentration of the hydronium ion (treated as an unknown variable in Eq (8)). The model proposed in this study considered the change in volume  $V_a$ , and in the concentrations of the ionic species (Sesp *i*), based on the effect of adding the reagent solution as described by Eqs. (9) and (10).

$$f(H^+) = [S_{NH_4^+}(S_{IN}, H^+) + H^+] - \left[ \frac{S_{Va^-}(S_{Va}, H^+)}{208} + \frac{S_{Bu^-}(S_{Bu}, H^+)}{160} + \frac{S_{Pr^-}(S_{Pr}, H^+)}{112} + \frac{S_{Ac^+}(S_{Ac}, H^+)}{64} + S_{OH^-}(H^+) + S_{HCO_3^-}(S_{IC}, H^+) + 2S_{SO_4^{2-}}(S_{H_2SO_4}, H^+) \right] \quad (8)$$

$$V_a^{j+1} = V_a^j + V_d \quad (9)$$

$$S_{esp\ i}^{j+1} = \frac{S_{esp\ i}^j V_a^j}{V_a^{j+1}} \quad (10)$$

$$V_{H_2SO_4}^{j+1} = V_{H_2SO_4}^j + V_d \quad (11)$$

here Sesp *i* stands for the ions concentration, in g COD  $L^{-1}$ , that is generated by the numerical solution of the ADM1; the ratios 1/208, 1/160, 1/112, and 1/64 serve as unit-conversion factors from g COD to mol;  $V_a$  is the sample volume;  $V_d$  is the volume of a drop of  $H_2SO_4$ ; and  $V_{H_2SO_4}$  is the volume of the reagent  $H_2SO_4$ , needed in the titration (all volume parameters are in ml).

The proposed alkalinity model allowed the evaluation of the total (TA), intermediate (IA), partial (PA), and bicarbonate-based (BA) alkalinities. The final  $pH_{alk}$  values are shown in Table 3S in Supplementary material section (as indicated in Figure 2S in the decision block) for the different types of titration and considerations on the assessment of the different alkalinities.

## 2.5 Co-digestion process stability analysis

The stability of the AD process was analyzed according to the statistical process control theory via the use of Shewhart control charts. A control chart for a variable of interest required the means and standard deviations. These were calculated using Eqs. (12) and (13), using data from a period where the process displayed the desired behavior. In this case, the range from day 38 to 57 was considered as the base case, since the pH of the system showed low variability.

$$\mu_j = n^{-1} \sum_{i=1}^n x_{i,j} \quad \forall j \quad (12)$$

$$\sigma_j = \sqrt{n^{-1} \sum_{i=1}^n (x_{i,j} - \mu_j)^2} \quad \forall j \quad (13)$$

where  $j$  is the process variable (pH in this work),  $i$  is a single data point in the sample,  $\mu_j$  is the sample mean;  $\sigma_j$  is the standard deviation of the  $j$ th variable;  $n$  the number of data points; and  $x_{i,j}$  is the  $i$ -th data point of the  $j$ -th variable in the sample.

The process data were plotted alongside a control (CL<sub>*j*</sub>), upper control (UCL<sub>*j*</sub>), and lower control lines (LCL<sub>*j*</sub>), which were calculated according to Eqs. (14). In these equations,  $\alpha$  is a positive constant that sets the limits in which the process variable can oscillate, where lower values can be used to achieve tighter process control. In this case, a value of  $\alpha=3$  was used, as this is the standard practice (Montgomery and Runger, 2002).

$$UCL_j = \mu_j + \alpha\sigma_j \quad \forall j \quad (14a)$$

$$CL_j = \mu_j \quad \forall j \quad (14b)$$

$$LCL_j = \mu_j - \alpha\sigma_j \quad \forall j \quad (14c)$$

Additionally, the process pH was modeled as the response of a first-order linear system to an impulse manipulation. Particularly, pH is one of the key parameters for the control of the AD process. A slight variation in its value resulted in an exponential change in the concentration of  $H^+$  protons, which may lead to considerable impacts over the process. Additionally, it serves to identify possible inhibitory scenarios (Siddique and Wahid, 2018; Rivas-García *et al.*, 2013), while it is relatively easy to determine

during the process (Draa *et al.*, 2015). A first-order linear system is represented by Eq. 15a.

$$\frac{dpH}{dt} + ApH(t) = Bu(t) \quad (15a)$$

$$s.t. \quad pH(t_0) = pH_0 \quad (15b)$$

where  $dpH/dt$  represents the rate of change of pH with respect to time,  $u$  is the manipulation to the system (corresponding to the daily feed of the reactor), and  $A$  and  $B$  are constant values. The initial condition establishes that at time  $t_0$  the system has a value  $pH_0$ ; without loss of generality, the initial condition can be assumed to take place at time  $t = 0$  and have a value of  $pH_0 = 0$ . In the case where the initial conditions are not zero, a linear transformation can be performed to bring them to the origin. In this case,  $u(t)$  represents the daily feed to the reactor. The daily feed into the reactor could be modeled as an impulse function,  $u(t) = \beta\sigma(t)$ . Since the time it takes to input the feed into the reactor is relatively short in comparison to a full day. Where  $\sigma(t)$  is the Dirac delta function and  $\beta$  is a constant value. In this work,  $\beta = 8$  g of feed  $d^{-1}$  was used, as this was the amount of VS daily feed to the reactor.

After taking the Laplace transform on Eq. 15a, considering the origin as the initial conditions, and rearranging the terms, the system is described by Eq. 16. Where  $s$  is the Laplace variable that results from mapping the equation from the real plane into the complex plane. In this form, the transfer function states how the pH changes to a change in the feed.

$$\frac{\widetilde{pH}(s)}{U(s)} = \frac{k}{\tau s + 1} \quad (16)$$

where  $k$  is the process gain, given by  $B/A$ , and  $\tau$  is the time constant of the process, given by  $1/A$ . The term  $\widetilde{pH}(s)$  is the Laplace transform of the deviation variable after a linear transformation to the original variable, namely  $\widetilde{pH}(t) = pH(t) - pH_0$ . A similar transformation was applied to all the variables in Equation 15. This transformation had the purpose of bringing the initial conditions to the origin, i.e.,  $t_0 = 0$  and  $\widetilde{pH}_0(t_0) = 0$ . Substituting the function for  $\widetilde{U}(s) = \beta$  and taking the inverse Laplace transform, the function that describes how the process pH deviates from its initial value is described by Eq. 17.

$$\widetilde{pH}(t) = \frac{\beta k}{\tau} e^{-t/\tau} \quad (17)$$

The final expression to obtain the process pH, considering an initial condition different than zero

is given by Eq. 18, after applying the inverse linear transformation given by  $pH(t) = \widetilde{pH}(t) + pH_0$ .

$$pH(t) = pH_0 + \frac{\beta k}{\tau} e^{-t/\tau} \quad (18)$$

According to the response function, after the feed, the system will spike to a new pH and will eventually come back to its original pH value. The magnitude of the spike and the time it takes to come back are determined by the process gain and the time constant. Eq. 18 was fitted to the experimental data considering two different periods, the first period covered from day 11 to 31, which encompasses the VW mono-digestion process. The second period occurred from day 37 to 59, covering the VW:CM co-digestion process. The values of the initial pH used for the model were  $pH_0 = 6.45$  for the first period and  $pH_0 = 6.30$  for the second period.

### 3 Results and discussion

#### 3.1 Substrate and inoculum characterizations

The results for the characterization of the inoculum, VW and CM substrates are shown in Table 1. The inoculum had high ash content. Probably due to its origin (sedimented active biomass from an industrial anaerobic reactor), and to the fact that a considerable part of the organic matter had been mineralized due to microbial degradation. The inoculum also had a high content of protein-based material, which is common in activated sludges (Frolund *et al.*, 1995). High protein content could be indicative of the presence of microorganisms, according to Durmaz and Sanin (2003). The CM co-substrate presented TS and VS contents that were in the range reported in the literature: TS was in the range of 4.1 - 13.7% and VS in the range of 68.6 - 83.6% TS (Ebner *et al.*, 2016; Callaghan *et al.*, 2002; Schoen *et al.*, 2009). The TS content of the VW was slightly below the values reported in the literature, namely 9.5 - 19.54% TS, while the VS was in the normal range of 84.72 - 98.2% of TS (Ebner *et al.*, 2016; Callaghan *et al.*, 2002; Schoen *et al.*, 2009). The variation in the values for these parameters for CM and VW, when compared to the results in other research works, could be caused by different factors, such as the type of diet of the livestock (Møller *et al.*, 2014), the water content, storage conditions (Niu *et al.*, 2017; Page *et al.*, 2015), and the procedure to collect the sample and its degradation (Page *et al.*, 2015).

Table 1. Fresh substrate and inoculum characterization.

Parameter	Unit	Inoculum	VW	CM
TS	%	4.248	7.29 ± 0.028	13.31 ± 0.314
VS	% TS	76.02 ± 1.89	94.14 ± 0.21	83.57 ± 0.27
Ash	% TS	23.98 ± 1.89	5.86 ± 0.21	16.43 ± 0.27
STS	g g TS <sup>-1</sup>	0.002	0.008	0.0005
DSS	g g TS <sup>-1</sup>	0.007	0.0005	0.0003
VFA <sup>1</sup>	g g VS <sup>-1</sup>	0.005	0.021	0.027
Fibers	g g VS <sup>-1</sup>	0.112	0.093	0.268
Carbohydrates	g g VS <sup>-1</sup>	0.186	0.706	0.447
Proteins	g g VS <sup>-1</sup>	0.569	0.137	0.103
Lipids	g g VS <sup>-1</sup>	0.024	0.02	0.016
N-NH <sub>3</sub>	g g TS <sup>-1</sup>	0.003	0.002	0.001
TKN	g g TS <sup>-1</sup>	0.69	0.021	0.014
Alkalinity <sup>1</sup>	mg CaCO <sub>3</sub> L <sup>-1</sup>	550 ± 71 <sup>3</sup>	210 ± 0.0 <sup>3</sup>	1900 ± 141 <sup>3</sup>
pH		8.47 ± 0.007 <sup>3</sup>	5.06 ± 0.014 <sup>3</sup>	7.75 ± 0.04 <sup>3</sup>

VW= Vegetable waste; CM= Cow manure; TS= Total solids; VS= Volatile solids; STS= Soluble total solids; DSS= Dissolved soluble solids; VFA= Volatile fatty acids; TKN= Total Kjeldahl nitrogen.

<sup>1</sup>Solution at 40 g VS L<sup>-1</sup>

The N-NH<sub>3</sub> concentration in the characterized substrates in this work and those reported in the literature varied considerably. These variations had been previously observed in other characterization works, as reported by (Li *et al.*, 2017).

In Table 1, the differences in the fiber and carbohydrates content (determined as cellulose and hemicellulose) between VW and CM were notorious. The high carbohydrate content in AD processes promotes high concentrations of VFA, eventually leading to acidification (García-Peña *et al.*, 2011). High fractions of fibers are characteristic of recalcitrant substrates, such as CM (Boe *et al.*, 2009).

The initial and feeding conditions for the ADM1 model are presented in the Table 4S of supplementary material. The individual values of  $f_{X_{espi\_Xc}}$ ,  $S_{IN}$ ,  $S_{su}$ ,  $S_{aa}$ , and VFA were calculated based on the information in Table 1 and Eqs. (3) - (5). The initial values for the different microbial groups present in the inoculum and the co-digestion of VW:CM stage were evaluated based on data available in the literature. For the modeling of the VW mono-digestion stage, it was considered that the substrate added to the reactor lacks active biomass, since it was made up of undecomposed vegetables.

### 3.2 Mathematical model validation

The incorporation of the co-digestion model to the ADM1 structure did not entail the addition of new

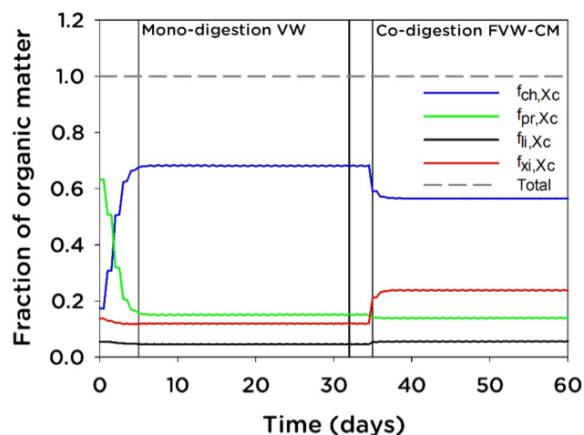
parameters. Additionally, the only changes in the value of the parameters (concerning the values proposed by Batstone *et al.*, (2002)) were the disintegration constant,  $k_{dis} = 1.6 \text{ d}^{-1}$ , and the carbohydrate hydrolysis constant,  $k_{hyd\_Xch} = 0.75 \text{ d}^{-1}$ .

Table 2 shows the value of the statistic parameter average absolute percentage deviation (AAPD) for the original ADM1 (Batstone *et al.*, 2002) and the proposed model, concerning the experimental data. It was observed that in the co-digestion period, the proposed model presented lower AAPD values for all parameters compared to the original ADM1; this strengthens the validity of the assumptions made in Section 2.3. Besides, in mono-digestion, the original ADM1 exhibited low goodness of fit for the total carbohydrates parameter. Both models had a low fitness in biogas productivity; during the first days of AD they were not able to predict the dynamic behavior (Figure 3).

The dynamic profile of the proximal composition ( $f_{X_{espi\_Xc}}$ ) of the organic matter in the reactive system is shown in Figure 1. During the stabilization period ( $t < 5 \text{ d}$ ) a fast increase in the carbohydrates fraction ( $f_{X_{ch\_Xc}}$ ) and a reduction on the protein fraction ( $f_{X_{pr\_Xc}}$ ) were observed. This behavior was due to the abundance of carbohydrates in the VW fed to the system (Table 4S), and the disintegration and hydrolysis of proteins. During the mono-digestion of VW, the organic matter composition remained stable.

Table 2. Average absolute percentage deviation (AAPD) for original ADM1 and its structural modification.

Parameter	AAPD of ADM1		AAPD of modified ADM1	
	Mono-digestion	Co-digestion	Mono-digestion	Co-digestion
VS	22.5	45.3	30.2	17.8
Total carbohydrates	96.4	97.2	30.1	49.7
Yield	85.6	95.8	93.8	27.9
Productivity	88.4	97.7	130	48.7
N-NH <sub>3</sub>	30.3	102.2	39.1	25
Acalinity	–	–	16.1	9.1


 Fig. 1. Dynamic profiles of the organic matter composition,  $f_{X_{espi}_{Xc}}$ , according to the mathematical model.

On the other hand, when the co-digestion started, the  $f_{X_{ch}_{Xc}}$  decreased considerably, while the inert matter fraction ( $f_{X_{li}_{Xc}}$ ) increased. This behavior was caused by the incorporation of CM in the feed, which is a substrate rich in compounds that can withstand the microbes' attack, effectively behaving as inert (fiber content, Table 1).

### 3.3 Co-digestion study

The behavior of the VS and carbohydrates inside the reactor is presented in Figure 2. No experimental data was taken during the stabilization period ( $t < 5$  d) since there was no effluent coming out of the reactor. Nonetheless, according to the model, there was a rapid decrease in the VS concentration (50% of degradation), which was in close agreement with the experimental data for days 1 and 5. The organic matter degradation could be due to the hydrolysis of proteins. The Tables 4S and 1 show that the initial composition in the reactor had a content of this material, which came from the inoculum. Furthermore, the profile

of  $f_{X_{pr}_{Xc}}$  in the organic matter dropped drastically during the five initial days, as shown in Figure 1. Additionally, the modeling results indicated that the insoluble organic matter lost a considerable portion of its proteinaceous material, from  $26 \text{ g L}^{-1}$  down  $1.7 \text{ g L}^{-1}$ , in the first five days.

The VS content predicted by the model during the intermediate stage (days 15 to 45 as shown in Figure 2) deviates from the experimental data. This behavior was probably due to the fact that the ADM1 considers that the disintegration and hydrolysis of the organic matter are independent of the colonization by hydrolytic bacteria (Mottet *et al.*, 2013). According to the model, during this period the concentration of fermenting microorganisms was higher. Shrestha *et al.* (2017) reported that these microorganisms were mainly made up of acid-producing bacteria and hydrolytic bacteria, which were responsible to a great extent of the hydrolysis process (Rivas-García *et al.*, 2020). A gradual increase of the VS concentration was observed after the VW:CM co-digestion period, caused by a high content of non-biodegradable lignocellulosic material present in the feed (Table 1). This phenomenon was linked with the increase of the recalcitrant matter fraction  $f_{X_{li}_{Xc}}$ , as shown in Figure 1.

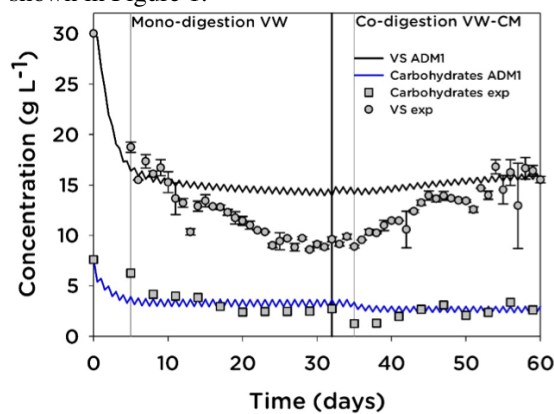


Fig. 2. Volatile solids (VS) and total carbohydrates profiles.

Table 3. Average values and standard deviations of the anaerobic digestion process' parameters in mono and co-digestion regime.

Parameter	Mono-digestion VW Period II	Co-digestion VW:CM Period III
Productivity ( $L\ biogas\ L\ digester^{-1}\ d^{-1}$ )	$0.850 \pm 0.282$	$0.965 \pm 0.196$
pH	$6.213 \pm 0.107$	$6.200 \pm 0.048$
Alkalinity ( $mg\ CaCO_3\ L^{-1}$ )	$4905 \pm 1772$	$3050 \pm 315$
CH <sub>4</sub> (%)	$44.8 \pm 3.27$	$44.9 \pm 4.22$

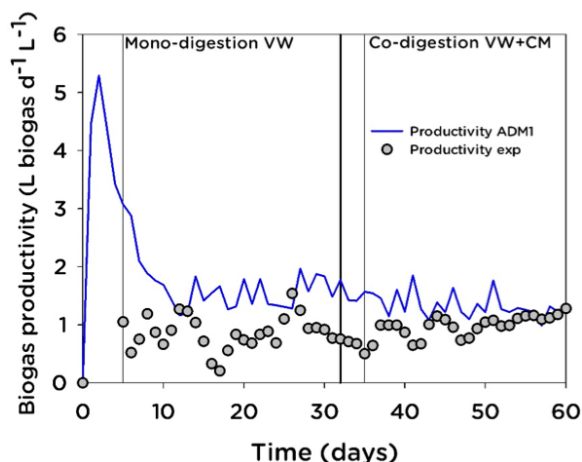


Fig. 3. Biogas productivity profile and control plots.

The insoluble carbohydrates concentration, which accounts for cellulose and hemicellulose, is presented in Figure 2. A decrease in the concentration was observed during the first 20 days, followed by a relatively constant concentration during the period of between days 21 to 31. During the co-digestion stage, the concentration decreased again. This behavior could also be observed in the results obtained via the proposed co-digestion model (Figure 1). Thus, the dynamic behavior of the carbohydrate's concentration could be accurately predicted by the ADM1 with the proposed modifications.

The experimental results and model predictions for productivity are presented in Figure 3. It could be observed that the model predicted a fast biogas production during the stabilization period of the digester ( $t < 5\ d$ ), which did not agree with the experimental data. This discrepancy was because of the ADM1 models the hydrolysis and degradation of soluble compounds via first-order kinetics and Monod and Michaelis-Menten kinetics, respectively. These kinetic models do not consider a stabilization period since they are unstructured models (Shuler and Kargi, 2002). After day 12, the model could predict more

accurately the digestion process.

The average values for the biogas productivity along with its standard deviation are presented in Table 3 among other parameters obtained experimentally for the mono-digestion (period II) and co-digestion (period III). It can be observed that productivity increased by 14% during co-digestion. Additionally, it is worth noting that the standard deviation for productivity, pH, and alkalinity decreased for co-digestion, which could be an indicator of a more stable process. This condition was fostered by the addition of CM in the feed. Figure 3 shows a sustained increase in biogas productivity, ranging from 0.73 to 1.28  $L\ biogas\ L\ digester^{-1}\ d^{-1}$  for the period of between days 47 to 60 of the co-digestion with CM.

The experimental and simulated alkalinity results for the digester are shown in Figure 4. As well as the ratio of intermediate and bicarbonate alkalinity (IA/BA), as predicted by the ADM1 following the methodology established by Ripley *et al.* (1986). Li *et al.* (2017) used the IA/BA ratio as an early warning indicator for AD of VW processes (in a CSTR). They found that values higher than 0.6 led to an acidification of the reactor and an abrupt drop of the pH due to the accumulation of acetate, propionate, butyrate, and valerate. According to Figure 4, the maximum value for the IA/BA ratio was 0.51 in the early stages of the process. Probably, because during this period the microorganisms of the inoculum were in a state of limited substrate. After the VW is added to the reactor there is a fast degradation of the organic matter, causing an accumulation of VFA, which in turn has an impact on the pH, as it can be observed in Figure 6, along with a spike in biogas productivity (Figure 3). Once the mono-digestion and co-digestion begin, the IA/BA ratio does not exhibit values that indicate a potential system failure; probably due the high content of ammonia released as a consequence of the degradation of protein (during mono-digestion); as well as the high alkalinity content and pH value in CM (during co-digestion).

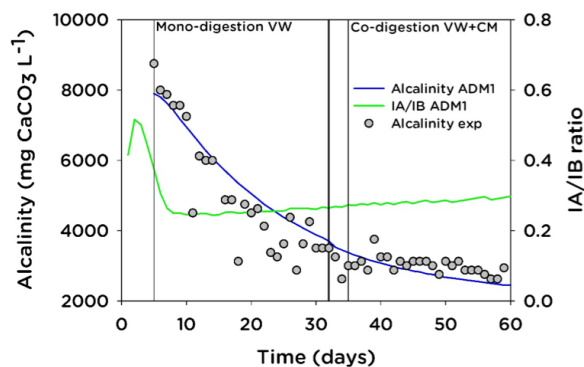


Fig. 4. Reactive medium alkalinity, ratio of the intermediate alkalinity (IA) with bicarbonate alkalinity (BA) and control plots.

The ammonia in an AD process originates from the degradation of proteins, peptides and amino acids, mainly. It plays an essential role in cell growth and the stabilization of pH by neutralizing the VFA. Boe (2006) stated that ammonia concentration, along with alkalinity and pH, were the parameters that helped assess the effectivity, and ensured good monitoring and control of AD processes. The total alkalinity profile and the  $\text{NH}_3$  content are shown in Figures 4 and 5, respectively. These graphs showed a constant decrease in both parameters for most of the process. Li *et al.* (2017) found a similar behavior, stating that it could be due to the lack of effluent recirculation in the reactive system. Similar to the system used in this work, causing a gradual loss of ammonia due to the system dilution, as the feed has a low ammonia concentration. It could be observed that the simulation results predicted the experimental behavior for the total alkalinity. In contrast, the  $\text{NH}_3$  showed a rapid accumulation and an early maximum value, in disagreement with the experimental data that displayed a latency period during the first 10 days. The ADM1 considers that the only source for  $\text{NH}_3$  generation is the acidogenesis of amino acids (mainly of alanine and glycine). The amino acid degradation is modeled via the coupled reactions of Stickland (Madigan *et al.*, 2006) that take place during the hydrolysis of proteins. These phenomena are modeled in the ADM1 via a group of microorganisms specifically associated with soluble amino acids, via Monod and Michaelis-Menten kinetics. These kinetic models were not able to predict the lag phase, which was the main cause of the deviation of the simulation results concerning the experimental data from days 10 to 32. The experimental values of  $\text{NH}_3$  during the co-

digestion displayed a slow decay, stabilizing around  $555 \text{ mg NH}_3 \text{ L}^{-1}$  for the last week of the experimental run. Li *et al.* (2017) found that for values under  $280 \text{ mg NH}_3 \text{ L}^{-1}$ , the inhibition of the reactive media due to excessive accumulation of VFA was fostered.

The experimental values of the alkalinity, in Figure 4, during the VW mono-digestion, displayed a decreasing trend, dropping from 8750 to  $3000 \text{ mg CaCO}_3 \text{ L}^{-1}$ , while presenting a high dispersion. This behavior could be observed by comparing the experimental values against the predicted profile (continuous line). On the other hand, the alkalinity showed a more stable behavior, staying in the range of between 2750 to  $3000 \text{ mg CaCO}_3 \text{ L}^{-1}$ , during the VW:CM co-digestion period.

The pH presented four characteristic behaviors, corresponding to the different feeding regimes to the reactor, as observed in Figure 6. During the period I, the process pH dropped sharply corresponding with the rapid decrease of VS, as observed in Figure 2. The simulated results pointed out that this behavior was related to the fast speed of hydrolysis for proteins and carbohydrates. These, in turn, resulted in a fast accumulation of VFA, showing a maximum value of  $3.57 \text{ g L}^{-1}$  during the second day of the process, and stabilizing around  $0.1 \text{ g L}^{-1}$  from day 7 to 32. The period covering the VW mono-digestion presented a decrease in the pH value with high instability in the system. This was because the formulation of vegetables fed to the reactor had  $40 \text{ g VS L}^{-1}$  with a pH value of 5.06, a relatively low alkalinity value of  $550 \text{ mg CaCO}_3 \text{ L}^{-1}$ , and a high content of carbohydrates,  $0.706 \text{ g g VS}^{-1}$ . All these factors increased the risk of acidification. At the end of period II, a pulse of sucrose (as described in Table 4S) was fed to the reactor.

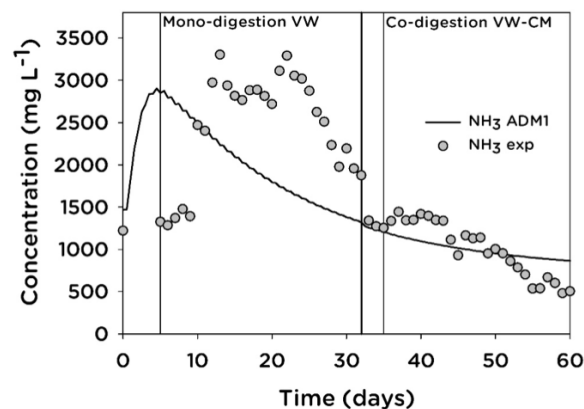


Fig. 5. Ammonia profile in the reactor.

Table 4. Shewhart's parameters and first order model parameters for the pH response data.

Parameter	Units	Mono-digestion	Co-digestion
<i>Shewhart's parameters</i>			
$\mu$	–	6.21	6.2
$\sigma$	–	0.1	0.04
UCL	–	6.33	–
CL	–	6.2	–
LCL	–	6.06	–
<i>First order model parameters for the pH response data</i>			
$k$	(g of feed/d) <sup>-1</sup>	-0.0177	-0.0137
$\tau$	d	0.5608	0.9595
$\beta$	g of feed d <sup>-1</sup>	8	8

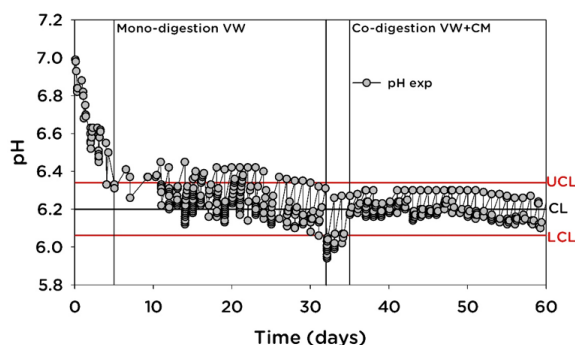
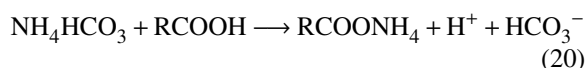
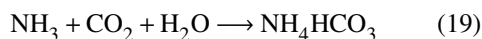


Fig. 6. Experimental behavior of the pH during the different substrate feed periods and control plots.

The response of the system to this perturbation was a sudden drop of the pH, down to a value of 5.94 as observed in Figure 6, a decrease of 1877 - 1340 mg of  $\text{NH}_3 \text{L}^{-1}$  (Figure 6), and a decrement in alkalinity (Figure 4). Li *et al.* (2017) mentioned that the fall of the ammonia nitrogen levels was due to the high content of soluble mono-saccharides. This was related to the sucrose catabolic reactions, since the sucrose is soluble and highly bioavailable, which generate VFA and  $\text{CO}_2$ . The ammonia in the solution reacted with the soluble  $\text{CO}_2$  in an irreversible reaction, creating ammonium carbonate ( $\text{NH}_4\text{HCO}_3$ ), which in turn reacted with the VFA to produce ammonium salts, as described by Eqs. (19) and (20).



The pH values for the VW:CM co-digestion period (III), oscillated less than for the VW mono-digestion. The addition of manure created a more stable reactive media while increasing biogas productivity.

The CM improved the buffering capacity of the system due to its high alkalinity (Gerardi, 2003), 1900 mg  $\text{CaCO}_3 \text{L}^{-1}$  (almost tenfold than VW), and to the fact that it had a pH = 7.75 (Table 1). The standard deviation for the pH during CM co-digestion (Table 3) exhibited a lower value compared to the VW mono-digestion period.

### 3.4 Stability analysis of the reactive system

The stability of the process was evaluated for two periods, the first one runs from day 11 to 31, which covers the VW mono-digestion, and the second period encompasses the VW:CM co-digestion process starting at day 37 and ending on day 59.

The average value and standard deviation for the pH, alongside the parameters used to construct the Shewhart control plots are presented in Table 4. It is worth noting that the standard deviation for the co-digestion period was consistently smaller than for the mono-digestion, which indicates less variability in the system.

The Shewhart control plots in Figure 6 shows the behavior of the pH. When the values fall outside the boundaries set by the UCL and LCL, it indicates a potential problem with the system. In the mono-digestion the pH values tended to fall outside the control boundaries, indicating that this parameter was less sensitive when cattle manure was added to the fed.

In Figure 3, the dispersion in the biogas productivity data in the mono-digestion period was notorious. This condition could be a result of the sensitivity of the methanogenic microorganisms to pH variations as mentioned by Gerardi (2003). During the co-digestion stage, the system pH presented less variability creating an environment conducive to less dispersion and even causing an increase in productivity (as shown in Figure 2 and Table 3).

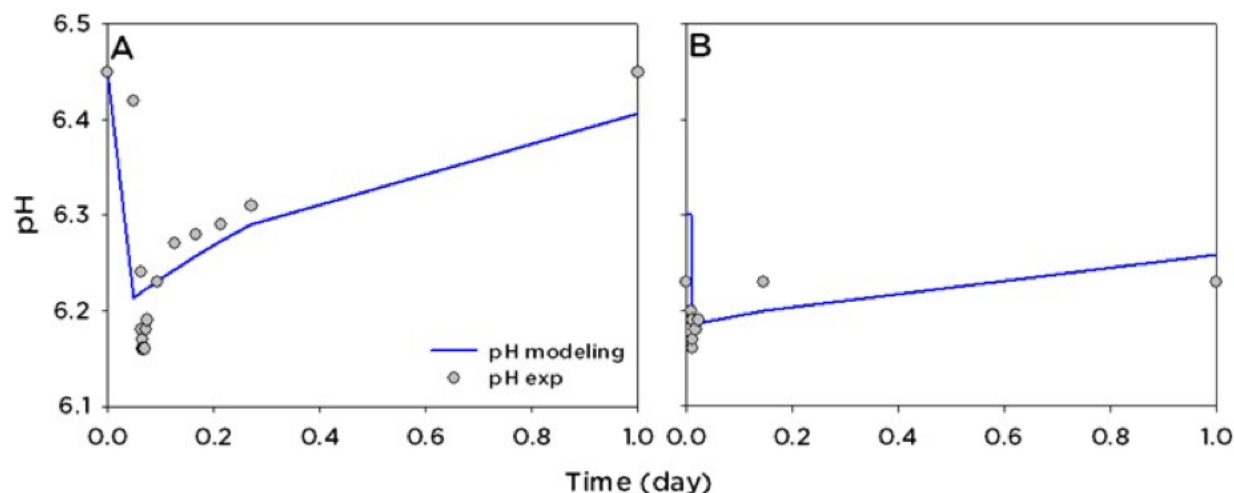


Fig. 7. Response of the pH to the daily feed under mono-digestion (day 18) and co-digestion (day 39). The solid lines represent the first order model response, and the dots represent the experimental data.

Thus, reinforcing the fact that having a good co-substrate, *e.g.* CM, improves the process stability by enhancing the buffering capacity of the reactive media.

In Table 4, the values of the process gain ( $k$ ) and time constant ( $\tau$ ) for the first-order model response of pH to an impulse input are presented. A bigger gain indicates a more abrupt change in the pH response to an input change, and a bigger time constant represents a slower response. The negative sign of the gain indicates that the pH will drop after the daily feed to the reactor. In this process, the gain was proportional to the carbohydrate content of the feed and inversely proportional to the alkalinity of the feed (see Table 1). In the AD process, these compounds generate a high concentration of VFA (the leading cause of pH decrease). The time constant was inversely proportional to ammonia content –which is considered as a buffer compound in the media (Meng *et al.*, 2018). During the mono-digestion process, the VW fed to the reactor had more than 70% of carbohydrates (VS basis), a pH of 5.06 and low alkalinity content, 200 mg CaCO<sub>3</sub> L<sup>-1</sup>, compared to 44% of carbohydrates (VS basis), a pH of 7.75, and an alkalinity of 1900 mg CaCO<sub>3</sub> L<sup>-1</sup> of the CM. The ammonia content, as shown in Figure 5, was higher during the AD stage and remained relatively constant at a lower value during the AcoD phase. Thus, the pH will drop abruptly and will have a faster recovery for the AD process, compared to the dynamic behavior of the co-digestion process.

Figure 7 shows an example of the dynamic behavior of the pH after the reactor was subjected to an impulse of feed for the VW mono-digestion

(day 18) and VW:CM co-digestion (day 39) process, respectively. The pH for the mono-digestion process dropped from 6.45 down to 6.19, while for the co-digestion the pH falls from 6.3 to 6.18. The slower response of the co-digestion process also helped attenuate the sensibility of the process, thus increasing its stability.

In this study, it was evident that in the process of mono and co-digestion of VW, low pH values persisted and that the addition of CM was not a factor that stimulated an increment in this parameter (as seen in Figure 6). However, the VW:CM co-digestion encouraged a system that had lower sensitivity to drops in the pH related to the feed. The VW are by their nature wastes that have a weekly and seasonal variability in their composition. An adequate biogas production process from VW would preferably require co-substrates that counterbalance these changes, keeping the parameters related to the digester stability outside the failure thresholds, as well as maintain stable or increasing biogas production, as seen in Figure 3. An alternative to operating a process with higher biogas productivity and pH at values close to optimal (6.8 - 7.2), is to start the VW:CM co-digestion process from the beginning.

## Conclusions

In this work, a co-digestion model based in the Anaerobic Digestion Model No.1 (ADM1), was developed. In it, the fractions of carbohydrates,

proteins, fats, and inerts were modeled as dynamic variables. The proposed model adequately predicted the behavior of volatile solids, total carbohydrates, total alkalinity, ammonia, biogas productivity, and different types of alkalinity (total, intermediate, bicarbonate, and partial) in a semi-continuous process of co-digestion of vegetable waste with cow manure (VW:CM). Compared to VW mono-digestion, VW:CM co-digestion decreased the standard deviation in pH variations, leading to a sustained increase in CH<sub>4</sub> productivity, and did not show a failure trend in the early warning indicator IA/BA (the relationship between intermediate alkalinity and bicarbonate alkalinity).

The stability analysis suggested that the addition of CM as a co-substrate in the anaerobic digestion of VW had a positive effect on the alkalinity, helping to attenuate the response of the process pH to the feed composition, and effectively creating a more stable reactive medium, which was conducive to fostering a sustained increase in biogas productivity.

Finally, the alkalinity and co-digestion model incorporated into the ADM1 structure allows the evaluation of conditions that promote sustainable biogas production. It was also demonstrated that the model could be used as a tool for the prevention of failures in anaerobic co-digestion processes of agroindustrial waste. This research could be extended by applying different rates of organic load to the anaerobic co-digestion process aiming at increasing biogas productivity, which could help the financial success of the process. A limitation of this work was that VW physical variability and bromatology were not evaluated, so their potential impacts on biogas productivity are still unknown. Future research could focus on the study of VW variability and its effect on anaerobic co-digestion processes. The analysis of co-substrates is also essential because it could avoid possible failures associated with the variability of these wastes.

### Acknowledgements

We want to thank the Food, Drug, and Toxicology Laboratory of the School of Chemical Sciences of the Universidad Autonoma de Nuevo Leon, as well as the Consejo Nacional de Ciencia y Tecnologia (CONACYT) for financing the project: CB-2015-254294.

### Nomenclature

$\mu_j$	sample mean
A	system's alkalinity, mg CaCO <sub>3</sub> L <sup>-1</sup>
CL <sub>j</sub>	alongside a control
esp <sub>i</sub>	concentration of specie <i>i</i> in the reactor output, g COD L <sup>-1</sup>
esp <sub>i,Co</sub>	concentration of specie <i>i</i> in the co-substrate, g COD L <sup>-1</sup>
esp <sub>i,IN</sub>	concentration of specie <i>i</i> in the reactor feed, g COD L <sup>-1</sup>
esp <sub>i,S</sub>	concentration of specie <i>i</i> in the substrate, g COD L <sup>-1</sup>
$\bar{f}_{X_{esp\ i,Xc}}$	fraction of insoluble particles <i>i</i> in the composite in the reactor, kgCOD <sub>X<sub>i</sub></sub> kgCOD <sub>X<sub>c-1</sub></sub>
$\bar{f}_{X_{esp\ i,Xc(Co)}}$	fraction of insoluble particles <i>i</i> in the composite in the co-substrate, kgCOD <sub>X<sub>i</sub></sub> kgCOD <sub>X<sub>c-1</sub></sub>
$\bar{f}_{X_{esp\ i,Xc(S)}}$	fraction of insoluble particles <i>i</i> in the composite in the substrate, kgCOD <sub>X<sub>i</sub></sub> kgCOD <sub>X<sub>c-1</sub></sub>
$\bar{f}_{X_{espi,Xc\ IN}}$	fraction of insoluble particles <i>i</i> in the composite in the feed, kgCOD <sub>X<sub>i</sub></sub> kgCOD <sub>X<sub>c-1</sub></sub>
<i>k</i>	process gain
LCL <sub>j</sub>	lower control lines
<i>n</i>	number of data points
N <sub>H<sub>2</sub>SO<sub>4</sub></sub>	normality of the solution of H <sub>2</sub> SO <sub>4</sub> , N
<i>q<sub>IN</sub></i>	flow rate in of the reactor, L d <sup>-1</sup>
<i>q<sub>OUT</sub></i>	flow rate out of the reactor, L d <sup>-1</sup>
<i>r<sub>S/Co</sub></i>	represents the substrate to co-substrate ratio
<i>S<sub>espi</sub></i>	ions concentration, g COD L <sup>-1</sup>
<i>t</i>	time, d
<i>U</i>	daily feed to the reactor
UCL <sub>j</sub>	upper control
<i>V<sub>a</sub></i>	sample volumen, mL
<i>V<sub>d</sub></i>	volume of a drop of H <sub>2</sub> SO <sub>4</sub> , mL
<i>V<sub>H<sub>2</sub>SO<sub>4</sub></sub></i>	volume of sulphuric acid solution used as reagent, mL
<i>V<sub>L</sub></i>	volume of the reactive medium, L
<i>X<sub>C</sub></i>	composite concentration in the reactor, g COD L <sup>-1</sup>
<i>X<sub>C,Co</sub></i>	composite concentration in the co-substrate, g COD L <sup>-1</sup>
<i>X<sub>C,IN</sub></i>	composite concentration in the feed, g COD L <sup>-1</sup>
<i>X<sub>C,S</sub></i>	composite concentration in the substrate, g COD L <sup>-1</sup>
<i>X<sub>i,j</sub></i>	<i>i</i> th data point of the <i>j</i> th variable in the sample

$\alpha$	positive constant
$\beta$	constant value
$\rho_{esp\ i}$	represents the kinetic rate of specie $i$ inside the reactor, as modeled by the ADM1
$\sigma_j$	standard deviation of the $j$ th variable
$\tau$	time constant of the process

## References

- Abubaker, J., Risberg, K. and Pell, M. (2012). Biogas residues as fertilisers - Effects on wheat growth and soil microbial activities. *Applied Energy* 99, 126-134.
- Aldana-Espitia, N. C., Botello-Álvarez, J. E., Rivas-García, P., Cerino-Córdova, F. J., Bravo-Sánchez, M. G., Abel-Seabra, J. E., and Estrada-Baltazar, E. (2017). Environmental impact mitigation during the solidwaste management in an industrialized city in Mexico: an approach of life cycle assessment. *Revista Mexicana de Ingeniería Química* 16, 562-580.
- Anderson, G.K. and Yang, G. (1992). Determination of bicarbonate and total volatile acid concentration in anaerobic digesters using a simple titration. *Water Environment Research* 64, 53-59.
- AOAC Official Methods of Analysis. (1998). In: *Association of Official Agricultural Chemists Volume 16th*. Gaithersburg, USA.
- AOAC Official Methods of Analysis. (1990). *AOAC Official Method 962.09*. In: *Association of Official Agricultural Chemists Volume 16th*. Gaithersburg, USA.
- APHA American Public Health Association. (1992). *Standard Methods for Examinations of Water and Wastewater*. Washington, D.C., USA.
- Arnell, M., Astals, S., Åmand, L., Batstone, D.J., Jensen, P.D. and Jeppsson, U. (2016). Modelling anaerobic co-digestion in Benchmark Simulation Model No. 2: Parameter estimation, substrate characterization and plant-wide integration. *Water Research* 98, 138-146.
- Astals, S., Ariso, M., Galí, A. and Mata-Alvarez, J. (2011). Co-digestion of pig manure and glycerine: Experimental and modelling study. *Journal of Environmental Management* 92, 1091-1096.
- Astals, S., Batstone, D.J., Mata-Alvarez, J. and Jensen, P.D. (2014). Identification of synergistic impacts during anaerobic co-digestion of organic wastes. *Bioresource Technology* 169, 421-427.
- Batstone, D.J., Keller, J., Angelidaki, I., Kalyuzhnyi, S.V., Pavlostathis, S.G., Rozzi, A. and Vavilin, V.A. (2002). *Anaerobic Digestion Model No. 1 (ADM1) Scientific and Technical Report No. 13*. London.
- Boe, K. (2006). Online monitoring and control of the biogas process. Technical University of Denmark.
- Boe, K. and Angelidaki, I. (2009). Serial CSTR digester configuration for improving biogas production from manure. *Water Research* 43, 166-172.
- Breeze, P. (2018). Landfill waste disposal, anaerobic digestion, and energy production. In: *Energy from Waste*, 39-47.
- Callaghan, F.J., Wase, D.A.J., Thayanithy, K. and Forster, C.F. (2002). Continuous co-digestion of cattle slurry with fruit and vegetable wastes and chicken manure. *Biomass and Bioenergy* 22, 71-77.
- CEDA. (2011). Central de Abastos de la Ciudad de Mexico. Electronic book. Chakraborty, D. and Mohan, S.V. (2018). Effect of food to vegetable waste ratio on acidogenesis and methanogenesis during two-stage integration. *Bioresource Technology* 254, 256-263.
- Cheng, H. and Hu, Y. (2010). Municipal solid waste (MSW) as a renewable source of energy: Current and future practices in China. *Bioresource Technology* 101, 3816-3824.
- De Baere, L. (2006). Will anaerobic digestion of solid waste survive in the future? *Water Science and Technology* 53, 187-194.
- Di Maria, F., Sordi, A., Cirulli, G. and Micale, C. (2015). Amount of energy recoverable from an existing sludge digester with the co-digestion with fruit and vegetable waste at reduced retention time. *Applied Energy* 150, 9-14.

- Draa, K.C., Voos, H., Darouach, M. and Alma, M. (2015). A Formal modeling framework for anaerobic digestion systems. *2015 17th UKSim-AMSS International Conference on Modelling and Simulation (UKSim)*, 426-431.
- Durmaz, B. and Sanin, F.D. (2003). Effect of carbon to nitrogen ratio on the physical and chemical properties of activated sludge. *Environmental Technology* 24, 1331-1340.
- Ebner, J.H., Labatut, R.A., Lodge, J.S., Williamson, A.A. and Trabold, T.A. (2016). Anaerobic co-digestion of commercial food waste and dairy manure: Characterizing biochemical parameters and synergistic effects. *Waste Management* 52, 286-294.
- Escamilla-Alvarado, C., Poggi-Varaldo, H.M. and Ponce-Noyola, M.T. (2017). Bioenergy and bioproducts from municipal organic waste as alternative to landfilling: a comparative life cycle assessment with prospective application to Mexico. *Environmental Science and Pollution Research* 24, 25602-25617.
- FAO Global food losses and food waste: Extent, causes and prevention. (2011). FAO. FAO statistical yearbook 2014. (2014). Asia and the Pacific Food and Agriculture FAO.
- Flores-Estrella, R. A., Estrada-Baltazar, A. and Femat, R. (2016). A mathematical model and dynamic analysis of anaerobic digestion of soluble organic fraction of municipal solidwaste towards control design. *Revista Mexicana de Ingeniería Química* 15, 243-258.
- Frolund, B., Griebe, T. and Nielsen, P. (1995). Enzymatic activity in the activated sludge flocmatrix. *Applied Microbiology and Biotechnology* 43, 755-761.
- García-Gen, S., Sousbie, P., Rangaraj, G., Lema, J.M., Rodríguez, J., Steyer, J.P. and Torrijos, M. (2015). Kinetic modelling of anaerobic hydrolysis of solid wastes, including disintegration processes. *Waste Management* 35, 96-104.
- García-Peña, E.I., Parameswaran, P., Kang, D.W., Canul-Chan, M. and Krajmalnik-Brown, R. (2011). Anaerobic digestion and co-digestion processes of vegetable and fruit residues: Process and microbial ecology. *Bioresource Technology* 102, 9447-9455.
- Gavilán, A., Escamilla-Alvarado, C., Martínez, M.A. and Ramírez, T. (2018). Municipal solid waste management. In: *Progress and Opportunities for Reducing Short-lived Climate Pollutants Across Latin America and the Caribbean*, (L.T. Molina ed.), Pp. 118-135. UNEP and Climate and Clean Air Coalition.
- Gerardi, M.H. (2003). *The Microbiology of Anaerobic Digesters*. John Wiley & Sons, Inc.
- Hartmann, H. and Ahring, B.K. (2006). Strategies for the anaerobic digestion of the organic fraction of municipal solid waste: an overview. *Water Science and Technology* 53, 7-22.
- Holm-Nielsen, J.B., Al Seadi, T. and Oleskowicz-Popiel, P. (2009). The future of anaerobic digestion and biogas utilization. *Bioresource Technology* 100, 5478-5484.
- Jiang, Y., Heaven, S. and Banks, C.J. (2012). Strategies for stable anaerobic digestion of vegetable waste. *Renewable Energy* 44, 206-214.
- Kafle, G.K., Bhattarai, S., Kim, S.H. and Chen, L. (2014). Effect of feed to microbe ratios on anaerobic digestion of Chinese cabbage waste under mesophilic and thermophilic conditions: Biogas potential and kinetic study. *Journal of Environmental Management* 133, 293-301.
- Knol, W., Van Der Most, M.M. and De Waart, J. (1978). Biogas production by anaerobic digestion of fruit and vegetable waste. A preliminary study. *Journal of the Science of Food and Agriculture* 29, 822-830.
- Li, D., Chen, L., Liu, X., Mei, Z., Ren, H., Cao, Q. and Yan, Z. (2017). Instability mechanisms and early warning indicators for mesophilic anaerobic digestion of vegetable waste. *Bioresource Technology* 245, 90-97.
- Li, L., He, Q., Wei, Y., He, Q. and Peng, X. (2014). Early warning indicators for monitoring the process failure of anaerobic digestion system of food waste. *Bioresource Technology* 171, 491-494.
- Lin, J., Zuo, J., Gan, L., Li, P., Liu, F., Wang, K. and Gan, H. (2011). Effects of mixture ratio on anaerobic co-digestion with fruit and vegetable waste and food waste of China. *Journal of Environmental Sciences* 23, 1403-1408.

- Madigan, M.T., Martinko, J.M. and Brock, T.D. (2006). *Brock Biology of Microorganisms*. Pearson Prentice Hall, Ed.
- Masebinu, S.O., Akinlabi, E.T., Muzenda, E., Aboyade, A.O. and Mbohwa, C. (2018). Experimental and feasibility assessment of biogas production by anaerobic digestion of fruit and vegetable waste from Joburg Market. *Waste Management* 75, 236-250.
- Mata-Alvarez, J., Dosta, J., Romero-Güiza, M.S., Fonoll, X., Peces, M. and Astals, S. (2014). A critical review on anaerobic co-digestion achievements between 2010 and 2013. *Renewable and Sustainable Energy Reviews* 36, 412-427.
- Mata-Alvarez, J., Llabrés, P., Cecchi, F. and Pavan, P. (1992). Anaerobic digestion of the Barcelona central food market organic wastes: Experimental study. *Bioresource Technology* 39, 39-48.
- Matheri, A.N., Ndiweni, S.N., Belaid, M., Muzenda, E. and Hubert, R. (2017). Optimising biogas production from anaerobic co-digestion of chicken manure and organic fraction of municipal solid waste. *Renewable and Sustainable Energy Reviews* 80, 756-764.
- Meng, X., Yu, D., Wei, Y., Zhang, Y., Zhang, Q., Wang, Z. and Wang, Y. (2018). Endogenous ternary pH buffer system with ammonia-carbonates-VFAs in high solid anaerobic digestion of swine manure: An alternative for alleviating ammonia inhibition? *Process Biochemistry* 69, 144-152.
- Norma Mexicana. (2013). NMX-AA-005-SCFI-2013. Análisis de agua - Medición de grasas y aceites recuperables en aguas naturales, residuales y residuales tratadas - Método de prueba. Normas Mexicanas. Dirección General de Normas.
- Møller, H.B., Moset, V., Brask, M., Weisbjerg, M.R. and Lund, P. (2014). Feces composition and manure derived methane yield from dairy cows: Influence of diet with focus on fat supplement and roughage type. *Atmospheric Environment* 94, 36-43.
- Montgomery, D.C. and Runger, G.C. (2002). *Probabilidad y Estadística Aplicadas a la Ingeniería*. Limusa ed.
- Mottet, A., Ramirez, I., Carrère, H., Déléris, S., Vedrenne, F., Jimenez, J. and Steyer, J.P. (2013). New fractionation for a better bioaccessibility description of particulate organic matter in a modified ADM1 model. *Chemical Engineering Journal* 228, 871-881.
- Niu, M., Appuhamy, J.A.D.R.N., Dungan, R.S., Kebreab, E. and Leytem, A.B. (2017). Effects of diet and manure storage method on carbon and nitrogen dynamics during storage and plant nitrogen uptake. *Agriculture, Ecosystems and Environment* 250, 51-58.
- Nopens, I., Batstone, D.J., Copp, J.B., Jeppsson, U., Volcke, E., Alex, J. and Vanrolleghem, P.A. (2009). An ASM/ADM model interface for dynamic plant-wide simulation. *Water Research* 43, 1913-1923.
- Norma Mexicana (1994). NOM-116-SSA1-1994. Determinación de humedad en alimentos por tratamiento térmico - método por arena o gasa. Normas Mexicanas. Dirección General de Normas.
- Norma Mexicana. (2009). NOM-242-SSA1-2009. Productos y servicios - productos de la pesca frescos, refrigerados, congelados y procesados - especificaciones sanitarias y métodos de prueba. Normas Mexicanas. Dirección General de Normas.
- Norma Mexicana. (2011). NMX-F-608-NORMEX-2011. Alimentos - determinación de proteínas en alimentos - método de ensayo (prueba). Normas Mexicanas. Dirección General de Normas.
- Norma Mexicana. (2013). NMX-F-607-NORMEX-2013. Alimentos - determinación de cenizas en alimentos - método de prueba. Normas Mexicanas. Dirección General de Normas.
- Page, L.H., Ni, J.Q., Zhang, H., Heber, A.J., Mosier, N.S., Liu, X. and Harrison, J.H. (2015). Reduction of volatile fatty acids and odor offensiveness by anaerobic digestion and solid separation of dairy manure during manure storage. *Journal of Environmental Management* 152, 91-98.
- Pavi, S., Kramer, L.E., Gomes, L.P. and Miranda, L.A.S. (2017). Biogas production from co-digestion of organic fraction of municipal

- solid waste and fruit and vegetable waste. *Bioresource Technology* 228, 362-367.
- Ripley, L.E., Boyle, W.C. and Converse, J.C. (1986). Improved alkalimetric monitoring for anaerobic digestion of high-strength wastes. *Water Pollution Control Federation* 58, 406-411.
- Rivas-García, P., Botello-Álvarez, J. E., Abel Seabra, J. E., da Silva Walter, A. C. and Estrada-Baltazar, A. (2015). Environmental implications of anaerobic digestion for manure management in dairy farms in Mexico: a life cycle perspective. *Environmental Technology* 36, 1-38.
- Rivas-García, P., Botello-Álvarez, J.E., Miramontes-Martínez, L.R., Cano-Gómez, J.J. and Rico-Martínez, R. (2020). New model of hydrolysis in the anaerobic co-digestion of bovine manure with vegetable waste: Modification of Anaerobic Digestion Model No. 1. *Revista Mexicana de Ingeniería Química* 19, 109-122.
- Rivas-García, P., Botello-Álvarez, J.E., Estrada-Baltazar, A. and Navarrete-Bolaños, J.L. (2013). Numerical study of microbial population dynamics in anaerobic digestion through the Anaerobic Digestion Model No. 1 (ADM1). *Chemical Engineering Journal* 228, 87-92.
- Rosen, C. and Jeppsson, U. (2006). *Aspects on ADM1 Implementation within the BSM2 Framework*. Lund, Sweden.
- Scano, E.A., Asquer, C., Pistis, A., Ortu, L., Demontis, V. and Cocco, D. (2014). Biogas from anaerobic digestion of fruit and vegetable wastes: Experimental results on pilot-scale and preliminary performance evaluation of a full-scale power plant. *Energy Conversion and Management* 77, 22-30.
- Schoen, M.A., Sperl, D., Gadermaier, M., Goberna, M., Franke-Whittle, I., Insam, H. and Wett, B. (2009). Population dynamics at digester overload conditions. *Bioresource Technology* 100, 5648-5655.
- Shrestha, S., Fonoll, X., Khanal, S.K. and Raskin, L. (2017). Biological strategies for enhanced hydrolysis of lignocellulosic biomass during anaerobic digestion: Current status and future perspectives. *Bioresource Technology* 245, 1245-1257.
- Shuler, M.L. and Kargi, F. (2002). *Bioprocess engineering: Basic concepts*. P. Hall Ed. Siddique, M.N.I. and Wahid, Z.A. (2018). Achievements and perspectives of anaerobic co-digestion: A review. *Journal of Cleaner Production* 194, 359-371.
- Tambone, F., Scaglia, B., D'Imporzano, G., Schievano, A., Orzi, V., Salati, S. and Adani, F. (2010). Assessing amendment and fertilizing properties of digestates from anaerobic digestion through a comparative study with digested sludge and compost. *Chemosphere* 81, 577-583.
- Wang, X., Li, Z., Bai, X., Zhou, X., Cheng, S., Gao, R. and Sun, J. (2018). Study on improving anaerobic co-digestion of cow manure and corn straw by fruit and vegetable waste: Methane production and microbial community in CSTR process. *Bioresource Technology* 249, 290-297.
- Xie, S., Hai, F.I., Zhan, X., Guo, W., Ngo, H.H., Price, W.E. and Nghiem, L.D. (2016). Anaerobic co-digestion: A critical review of mathematical modelling for performance optimization. *Bioresource Technology* 222, 498-512.
- Zaher, U., Li, R., Jeppsson, U., Steyer, J.P. and Chen, S. (2009). GISCOD: General integrated solid waste co-digestion model. *Water Research* 43, 2717-2727.
- Zeynali, R., Khojastehpour, M. and Ebrahimi-Nik, M. (2017). Effect of ultrasonic pre-treatment on biogas yield and specific energy in anaerobic digestion of fruit and vegetable wholesale market wastes. *Sustainable Environment Research* 27, 259-264.